

## 11 – 6 Instantaneous Tracking of Earthquake Growth With Elasto-Gravity Signals in Japan and Application to Historical Data from the Tohoku Oki Earthquake.

ROUET-LEDUC Bertrand (DPRI, Kyoto University)

Rapid and reliable magnitude estimation for large earthquakes ( $M_w \geq 8$ ) is key to mitigate the risk associated with strong shaking and tsunamis. Early warning systems based on seismic waves often fail to rapidly estimate the size of very large earthquakes, and tend to saturate and be unable to distinguish between  $M_w 8$  earthquakes and  $M_w 9$  earthquakes. GNSS-based approaches can provide better estimations, but suffer from large uncertainties and latency associated with the slowness of seismic waves, and require to make a priori constraints that may be difficult to determine. The recently discovered speed-of-light Prompt Elasto-Gravity Signals (PEGS) has raised hopes to overcome these limitations, but has never been tested for operational early warning, in part to the very low signal to noise ratio they suffer from. In this research, PEGS is used in real-time to track earthquake growth without delay once the event reached a certain magnitude. A deep learning model is developed that leverages the information carried by PEGS recorded by regional broadband seismometers in Japan before P-waves. After training on a database of synthetic waveforms augmented with empirical noise, the first example of instantaneous tracking of an earthquake source time function is presented on real data. This model unlocks real time access to the rupture evolution of large earthquakes using a portion of seismograms that is routinely treated as noise, and could immediately be used to supplement existing methods, by refining  $M_w$  estimates for very large earthquakes.

Because of the rarity of PEGS observations (they are only observed for very large earthquakes), PEGSNet is trained on a database of synthetic PEGS waveforms to which real noise recorded at each station in the seismic network is added. The training database is made of 500,000 synthetic earthquake sources distributed along the Japanese megathrust, with location, strike and dip angles following the Slab2.0 model. Random magnitude and rake angles are drawn. The Gutenberg-Richter distribution for  $M_w$  is deliberately not used, to avoid sampling bias during training.

Random source time functions (STF) are generated using a model designed to mimic empirical laws and statistical observations to produce three-component waveforms representing the source characteristics of all expected large megathrust earthquakes along the Japanese subduction zone. Empirical noise recorded at each station is then added to the generated waveforms.

PEGSNet is a deep convolutional neural network (CNN) that combines convolutional layers and fully connected layers in sequence (Fig. 1).  $M_w$  is time-dependent, therefore noted as  $M_w(t)$ , and corresponds to the equivalent time-integrated STF at a given time. In order for PEGSNet to learn  $M_w(t)$ , it is given the network-wide data for 300 seconds and is tasked with estimating  $M_w(t)$  at the end of this 300 seconds window, that parses the data, as explained in Fig. 2.

Figure 3 summarizes the results on the synthetic test set (data the model has never seen in training) for estimating  $M_w(t)$  using PEGSnet. For each example in the test set, the end time of the input data is shifted with a time step of 1 s from the earthquake origin time ( $t=0$ ) to  $t=315$  s, and PEGSNet predicts  $M_w$  at each

time step. In other words, a running time window of 315 s parses the data, and is fed to PEGSNet, that makes its  $M_w(t)$  estimate for the end of the window.

In addition, PEGSNet makes a prediction only if at least 10 stations are active at a given time and a successful prediction is defined as within  $\pm 0.4$  magnitude units from the ground truth. Figure 3a indicates that PEGSNet is able to track the moment released by earthquakes with final  $M_w$  above 8.5/8.6 with good accuracy (above 90%) and low errors (below 0.25 in Fig. 3b), starting roughly after 40 s from origin time. For earthquakes with final  $M_w$  between 8.1 and 8.6, early tracking of the moment release is more difficult and only the final  $M_w$  can be estimated (with accuracy around 75% and errors above 0.25) after 150 s from origin time. Any predicted  $M_w$  below 8.1 is poorly constrained by the data. A conservative lower limit on PEGSNet sensitivity to  $M_w$  is between 8.0 and 8.2.

In order to examine the time-dependent performance of PEGSNet more closely, Figure 3c shows all the predictions (on the test set) associated with events with a final  $M_w$  of  $9.0 \pm 0.05$ . The system latency of about 30 s is related to the ten-station constraint and to the initial lack of PEGS sensitivity below  $M_w(t)=8.1$ . However, after 40 s (when the true  $M_w$  is generally above 8.0 according to the STF database) PEGSNet is able to track the evolution of the moment release instantaneously as indicated by the mode of the distribution of the predictions. These results show that PEGSNet is able to exploit the key features of PEGS data: 1) PEGS sensitivity to magnitude for large earthquakes allows the model to distinguish between a  $M_w = 8$  and a  $M_w = 9$  earthquake and 2) the information about  $M_w$  is effectively propagated at the speed of light, which results in instantaneous tracking of the moment release. Although P-wave triggering is needed at each station (and therefore some latency in the system exists), the instantaneous information about the source (carried by PEGS at the speed of light) is readily available in the pre P-wave time window. This allows PEGSNet to estimate  $M_w(t)$  with zero delay once the magnitude exceeds  $\sim 8.3$ .

PEGSNet has been tested on real data from the 2011  $M_w=9.0$  Tohoku-Oki earthquake (Fig. 4). The raw seismograms are processed as described in Vallée et al.<sup>1</sup> and fed to PEGSNet. As for the test set, a  $M_w$  prediction is made at each time step starting at the earthquake origin time. Figure 4a shows the results of this retrospective analysis compared with a “true” STF calibrated against a variety of different data types<sup>2</sup>. PEGSNet is able to instantaneously track the evolving moment release of the Tohoku earthquake, starting at about 55 s from origin time when  $M_w$  is about 8.2. PEGSNet reaches a correct prediction of the final  $M_w$  around 150 s when the rupture is over. Note that the predicted values are almost constant after 150 s, although new stations are added to the input data until 176 s after origin time (Fig. 4c). This highlights the robustness of the prediction even with an incomplete dataset. Consistently with synthetic tests (Fig. 3), predictions after 55 s (corresponding to the time the earthquake reaches  $M_w \sim 8.3$ ) provide robust snapshots of the evolution of the source at that exact time because PEGS carries information about the source at the speed of light.

To assess the robustness of the model’s  $M_w$  estimation on the Tohoku data, a test is performed in which the P-wave arrivals information is kept but the actual recorded waveforms in the pre P-wave time window is substituted with noise, and the resulting prediction of  $M_w(t)$  never exceeds the lower sensitivity limit of PEGSNet (i.e. 8.1) and remains constant at about 6.5, which provides a baseline value for noise.

PEGSNet requires few modifications to be implemented in real time. Predictions are fast to obtain, but some latency may be introduced by the preprocessing step. The model relies on P-wave arrival times which are assumed to be known, but any existing triggering algorithms can be used before feeding the data to the model.

These results provide the first example of instantaneous tracking of moment release for large earthquakes and promote PEGS data as a new class of observables for practical application in early warning systems, which are intrinsically limited by the speed of P-waves. For this reason, to-be-developed holistic approaches to EEWS that leverage the benefit of multiple data types may consider the advantage of including PEGS data.

In general, PEGSNET could come in complement to existing EEW warning systems, and would provide additional and independent estimates for very large magnitudes. Moreover, PEGSNet could immediately prove useful for tsunami early warning for which Mw estimation within a few minutes is vital.

This research has been published in:

Licciardi, A., Bletery, Q., Rouet-Leduc, B., Ampuero, J. P., & Juhel, K. (2022). Instantaneous tracking of earthquake growth with elastogravity signals. *Nature*, 606(7913), 319-324.

ROUET-LEDUC Bertrand

Other references:

1. Vallée, M. et al. Observations and modeling of the elastogravity signals preceding direct seismic waves, *Science*, **358**(6367), 1164-1168 (2017).
2. Bletery, Q. et al. A detailed source model for the M w 9.0 Tohoku-Oki earthquake reconciling geodesy, seismology, and tsunami records. *J. Geophys. Res. Solid Earth*, **119**, 7636-7653 (2014).

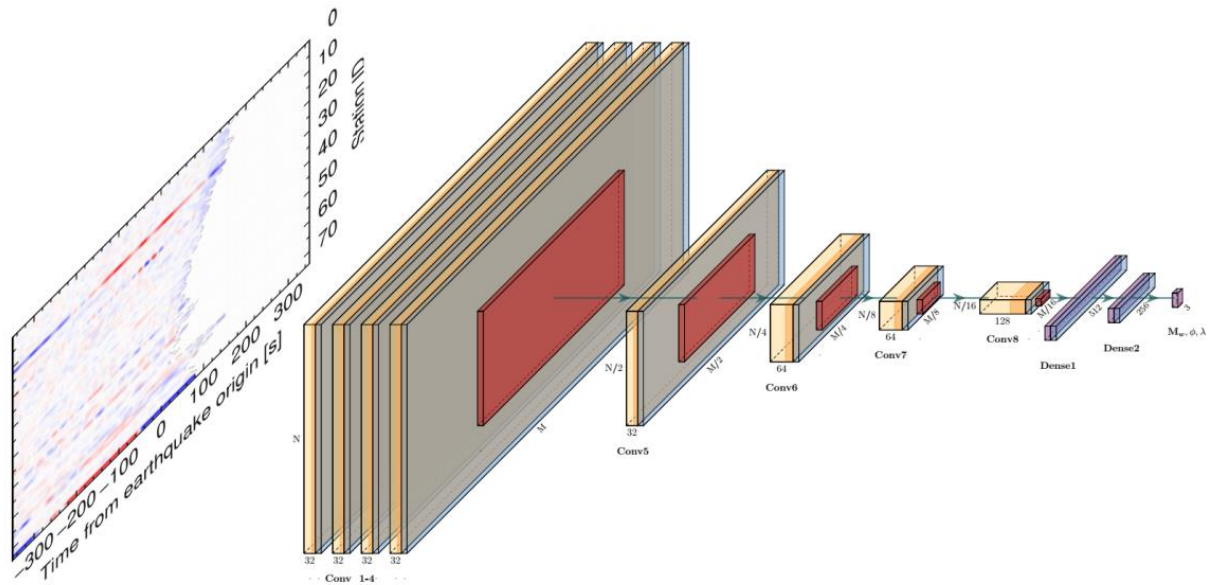


**Figure 1 | PEGSNet architecture.** The input data for one example consists in a three channel image of shape  $M \times N$ , where  $M$  is the number of time samples and  $N$  is the number of seismic stations. Only the vertical component of the input data is displayed for simplicity. Each convolutional block is composed of a convolutional layer (yellow) with a ReLu activation (orange), a spatial dropout layer (light blue). Max pooling layers (red) reduce each dimension of the input data by a factor of two. The number of filters used in each convolutional layer is indicated for clarity. The last convolutional block is connected to dense layers (purple) (using a ReLu activation function), with dropout (light blue). The output layer estimates  $M_w$ , latitude ( $\phi$ ) and longitude ( $\lambda$ ).

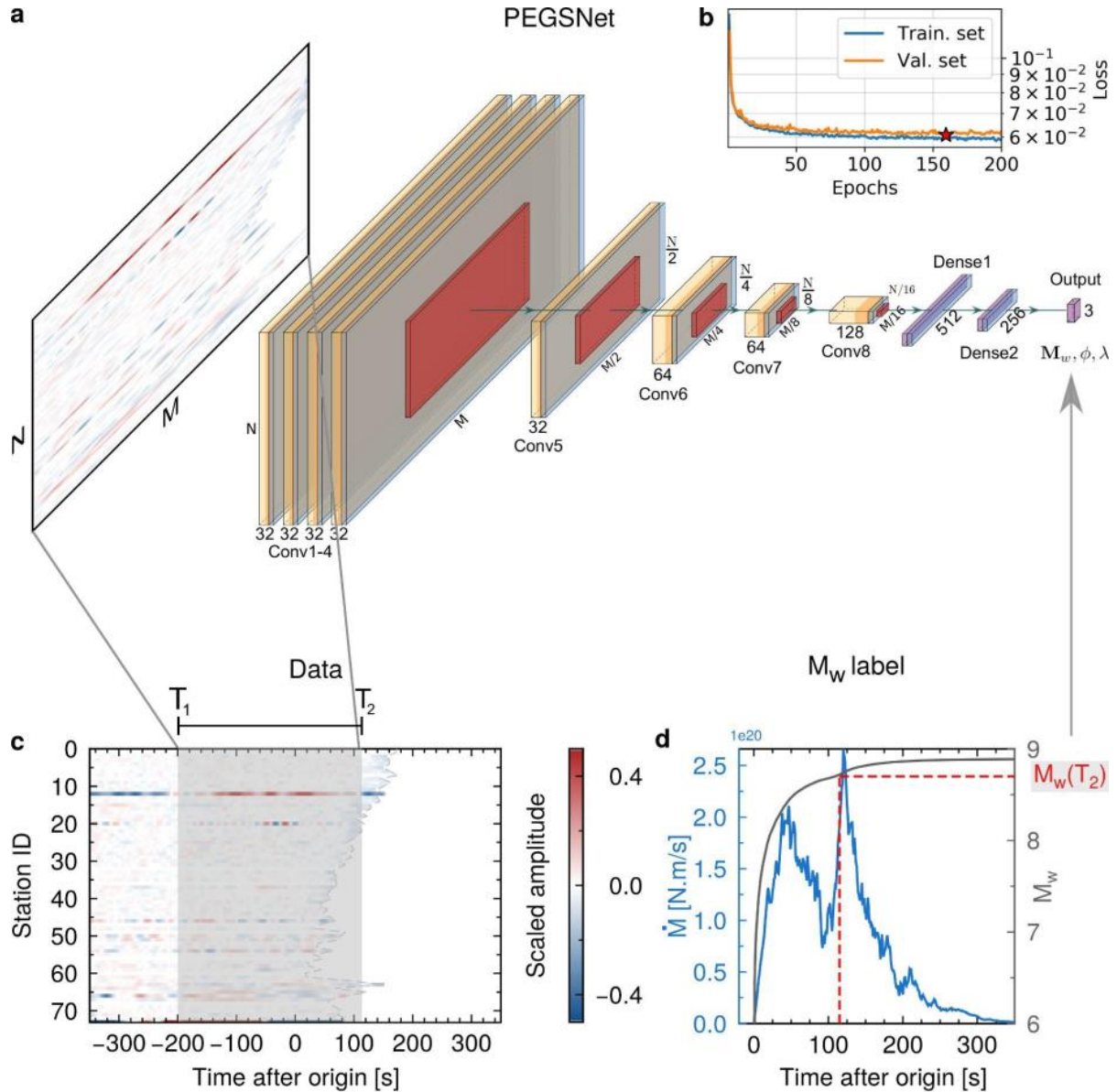


**Figure 2 | PEGSNet training strategy.** **a**, The input data for one example consists in a three-channel image of shape  $M \times N$ , where  $M$  is the number of time samples and  $N$  is the number of seismic stations. Only the vertical component of the input data is displayed for simplicity. Each convolutional block is composed of a convolutional layer (yellow) with a ReLu activation (orange), a spatial dropout layer (light blue). Max pooling layers (red) reduce each dimension of the input data by a factor of two. The number of filters used in each convolutional layer is indicated for clarity. The last convolutional block is connected to dense layers (purple) (using a ReLu activation function), with dropout (light blue). The output layer uses a tanh activation function to predict values of  $M_w$ , latitude ( $\phi$ ) and longitude ( $\lambda$ ). **b**, The value of the Huber loss is plotted as a function of epochs for the training and validation sets. The red star indicates the epoch with the minimum value of the loss on the validation set and the corresponding model is used for predictions on the test set and real data. **c**, Data from one example from the training database (vertical component). The grey shaded area corresponds to the input data for PEGSNet shown in (a).  $T_1$  and  $T_2$  are the beginning and end of the selected input window. During training,  $T_1$  is selected at random and  $T_2 = T_1 + 315$  s. **d**, Moment rate (blue) and  $M_w(t)$  (dark grey) for the selected event. Given the randomly selected value for  $T_1$  for this example, the corresponding label is  $M_w(T_2)$ , i.e. at the end of the selected window. This is compared with the predicted  $M_w$  estimated by PEGSNet in a and used for training.

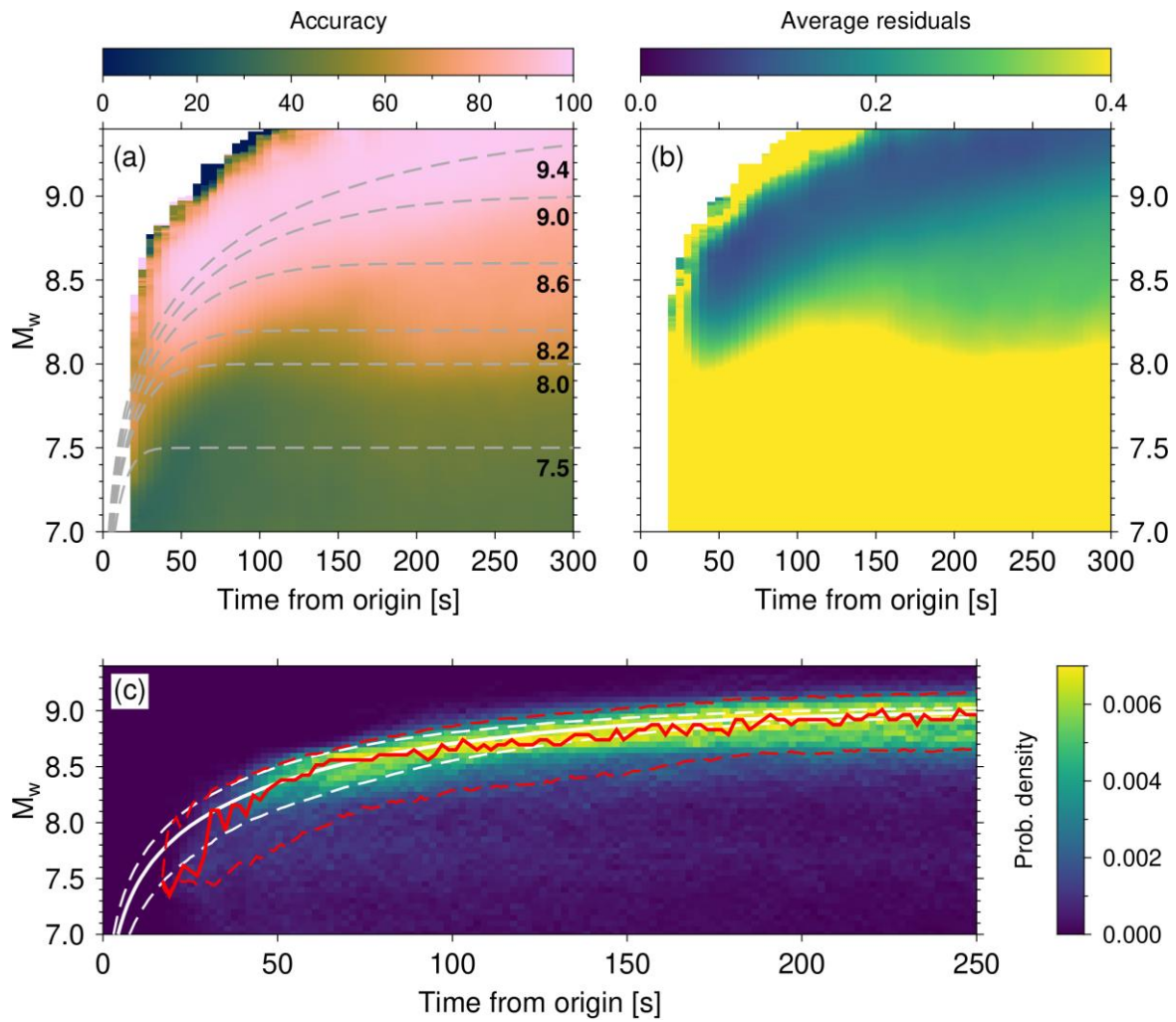


**Figure 3 | Timeliness of  $M_w$  estimation from PEGS data.** Results of predictions on the test set. (a) Model accuracy as a function of time and  $M_w$ . For each pixel in the image, accuracy is calculated as the number of successful predictions divided by the total number of samples. A prediction is defined successful if the distance with the ground truth is within  $\pm 0.4$  magnitude units. Dashed lines indicate the average values of the ground truth  $M_w(t)$  for events with different final magnitude the lower limit of PEGSNet sensitivity is between 8.0 and 8.2. (b) Same as in (a) but the average residuals ( $|M_w[\text{true}] - M_w[\text{pred}]|$ ) for each pixel are shown. (c) Probability density of  $M_w$  predictions for all the events in the test set with true final  $M_w$  of  $9 \pm 0.05$ . The solid red line is the mode of the distribution. The red dashed lines bound the 95-25 interquartile range. The white lines are the mean (solid) and the 95-5 interquartile range (dashed) of the ground truth.

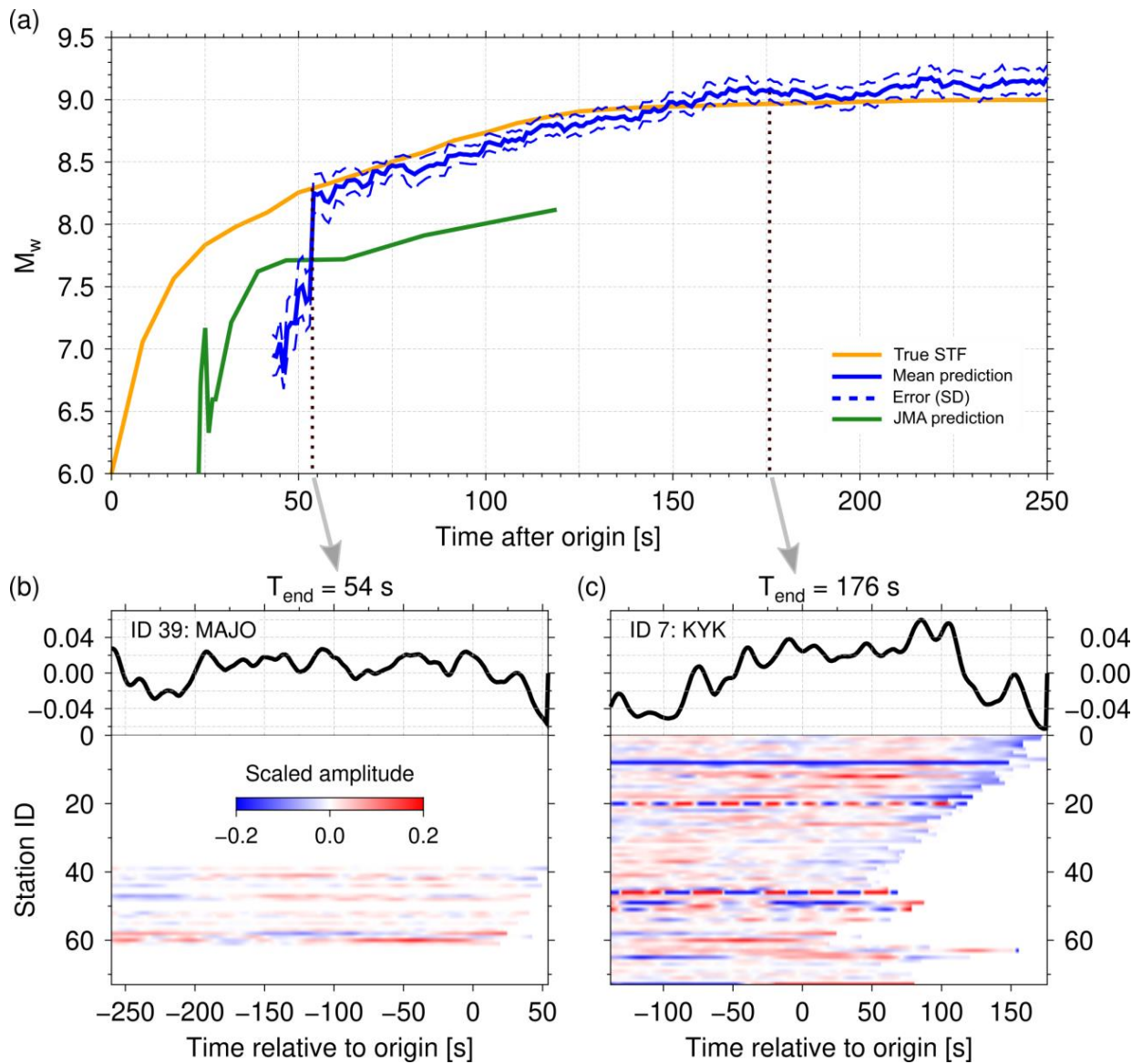


**Figure 4 | Instantaneous moment tracking of the 2011 Mw=9.0 Tohoku-Oki earthquake.** (a) PEGSNet  $M_w(t)$  predictions are represented by the mean (solid blue line) and one standard deviation (dashed blue lines) of the posterior distribution of the predictions at each time step. Predictions are displayed only if ten stations are available at a given time. The source time function of the Tohoku-Oki earthquake (orange line) is taken from Blettery et al.<sup>2</sup>. (b) and (c), PEGSNet input data (vertical component) at time steps of 54 and 176 s respectively. The top panels show the waveform of the last stations included in the input data at the corresponding time step.